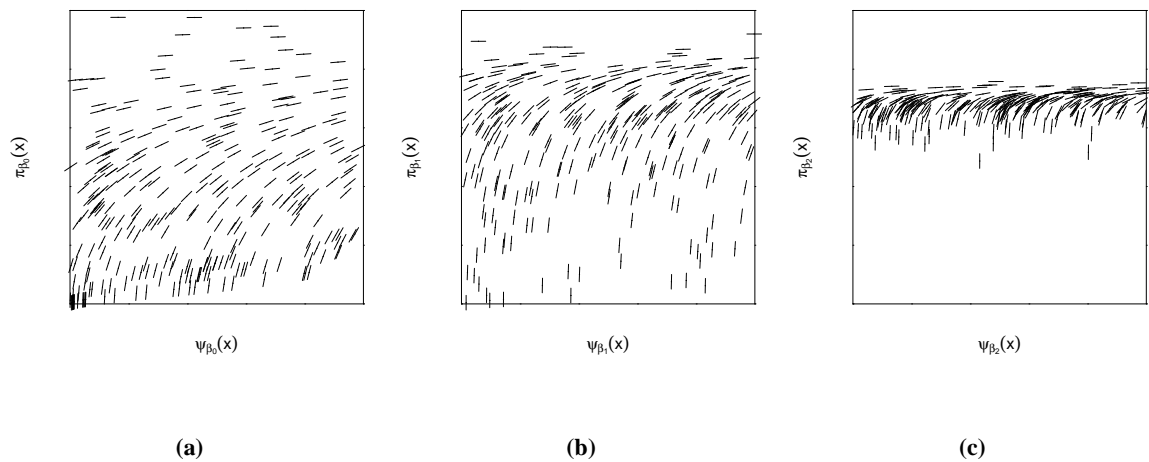


## Section 3.2 (SAVIAH)

To examine sensitivity of the local critique plots of the SAVIAH application to minor modifications or elaborations of the model, we consider two alternative model formulations, called SAVIAH2 and SAVIAH3.

### SAVIAH2

The prior choice that each of the three risk categories contribute with equal fractions of the overall disease rate is somewhat arbitrary and may be too influential. We now imagine having prior information on the means for  $\beta_0$ ,  $\beta_1$  and  $\beta_2$ , which happen to correspond to the fractions of disease rates attributed aposteriori to each risk category by the original model. This is achieved by setting  $\tau_0 = \frac{15\alpha_0}{Y}$ ,  $\tau_1 = \frac{5.4\alpha_1\bar{Z}}{Y}$  and  $\tau_2 = \frac{1.4\alpha_2}{Y}$ . Of course, the variances are also affected by this change. The local prior variances of  $\beta_0$  and  $\beta_1$  decrease, while the variance of  $\beta_2$  increases. The  $\pi$  and  $\psi$  functions are the same as for the original SAVIAH model, as seen in the paper. The local critique plots for this alternative model (SAVIAH2) can be seen in Figure 1 and 2. We see that the marginal posterior distributions of  $\beta_0$  and  $\beta_1$  are now using almost all of their local priors. The posterior samples of  $\beta_2$  are still located only in a small part of its local prior, but not as far out in the tail as before. The marginal posterior distribution of  $\beta_0$  has changed substantially compared to the one for the original SAVIAH model, with the posterior mean, median and standard deviation approximately halved from SAVIAH to SAVIAH2. The marginal posterior distributions of  $\beta_1$  and  $\beta_2$  are relatively unchanged (results not shown). The local critique plots for the  $\gamma_j$ 's are very similar to those seen for SAVIAH in the paper.



**Figure 1:** The local critique plots for (a)  $\beta_0$ , (b)  $\beta_1$  and (c)  $\beta_2$  for SAVIAH2 ( $M = 20000$ , results are shown for a random subsample of size 300).

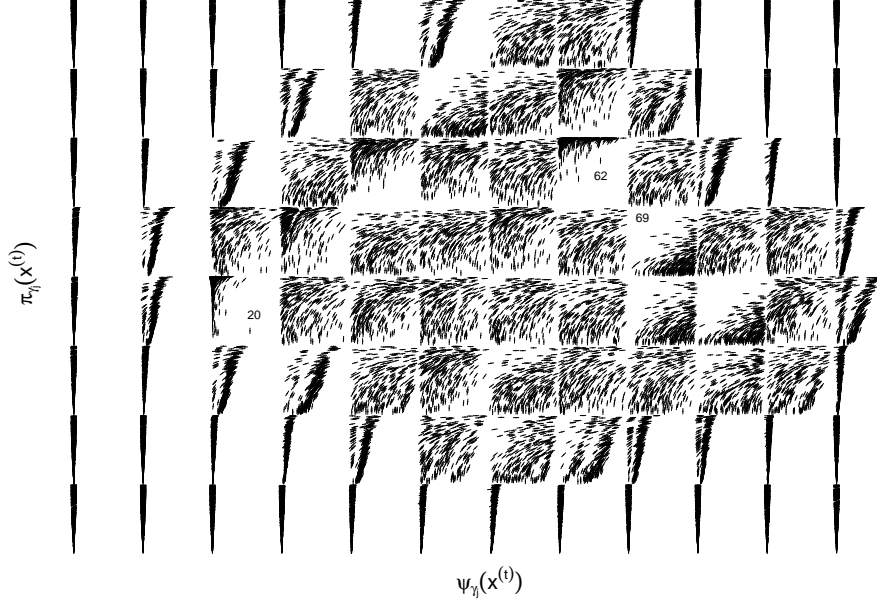


**Figure 2:** The local critique plots for  $\gamma_j$  for SAVIAH2 ( $M = 20000$ , results are shown for a random subsample of size 300). The plots for the latent risk areas are laid out according to the respective locations.

### SAVIAH3

It may be too restrictive to assume that all the  $\gamma_j$ 's come from the same distribution. We therefore consider a second alternative model, where we replace the fixed parameter  $\tau_\gamma$  in the local prior for  $\gamma_j$  by a random parameter  $\tau_{\gamma,j}$

$$(1) \quad \begin{aligned} \gamma_j &\sim \text{Ga}(\alpha_\gamma, \tau_{\gamma,j}), \quad j = 1, \dots, J \\ \tau_{\gamma,j} &\sim \text{Ga}(4, 4), \quad j = 1, \dots, J. \end{aligned}$$

Furthermore, we keep  $\alpha_\gamma = |B_j|/\text{km}^2$ . The other model choices are the same as those in Best, Ickstadt, Wolpert, and Briggs (2000). New  $\pi$  functions for the  $\gamma_j$ 's as well as  $\pi$  and  $\psi$  functions for  $\tau_{\gamma,j}$  are

$$(2) \quad \begin{aligned} \pi_{\gamma_j}(x) &= \Gamma(\gamma_j; \alpha_\gamma, \tau_{\gamma,j}) \\ \pi_{\tau_{\gamma,j}}(x) &= \Gamma(\tau_{\gamma,j}; 4, 4) \\ \psi_{\tau_{\gamma,j}}(x) &= \Gamma(\tau_{\gamma,j}; \alpha_\gamma + 1, \gamma_j). \end{aligned}$$

The rest of the  $\pi$  and  $\psi$  functions are the same as for SAVIAH in the paper. The local critique plots for this third model (SAVIAH3) can be seen in Figures 3, 4 and 5.

The (central)  $\gamma_j$ 's are now using more of their local priors and lifted likelihoods than what was the case for SAVIAH in the paper, this is also the case for  $\gamma_{20}$ ,  $\gamma_{62}$  and  $\gamma_{69}$ . The posterior quantiles of  $\gamma_{20}$ ,  $\gamma_{62}$  are much higher than for the original SAVIAH model, while the posterior quantiles of  $\gamma_{69}$  are a bit lower than for

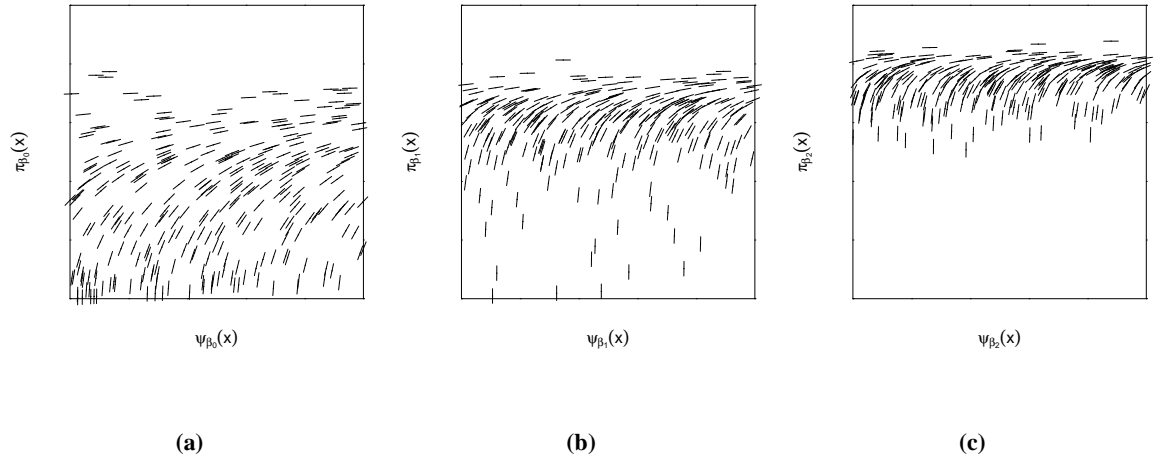


**Figure 3:** The local critique plots for (a)  $\beta_0$ , (b)  $\beta_1$  and (c)  $\beta_2$  for SAVIAH3 ( $M = 20000$ , results are shown for a random subsample of size 300).

SAVIAH. The pattern of  $\xi$  is more irregular than in Figure in the paper. This reflects the fact that the  $\pi_{\gamma_j}(x)$  for SAVIAH3 depend on the random parameter  $\tau_{\gamma_j}$ , while for SAVIAH  $\gamma_j$  was the only random component in  $\pi_{\gamma_j}(x)$ . Almost all the  $\tau_{\gamma_j}$ 's are using most of their local priors and lifted likelihoods. This is due to the fact that the local prior and the lifted likelihood for most  $\tau_{\gamma_j}$  agree quite well. Some  $\tau_{\gamma_j}$  have more noticeable plots. A high value of  $\gamma_j$  causes the lifted likelihood of  $\tau_{\gamma_j}$  to be narrow and at the same time have a location that disagrees with the local prior. This can be seen clearly for  $j = 20$  and  $j = 62$ , where the lifted likelihoods dominate the local priors.  $\gamma_{20}$  and  $\gamma_{62}$  have the highest  $\gamma_j$  posterior quantiles.

There is also an implicit effect on the local critique plots for  $\beta_0$ ,  $\beta_1$  and  $\beta_2$  from changing the local prior specification on the  $\gamma_j$ 's. The plots in Figure 3 differ from those for the SAVIAH model in the paper, even though the local priors for these parameters are the same as in the SAVIAH model. The most striking difference is perhaps that  $\beta_2$  is using more of its local prior.

## References

Best, N. G., Ickstadt, K., Wolpert, R. L., and Briggs, D. J. (2000). "Combining models of health and exposure data: the SAVIAH study", in *Spatial Epidemiology: Methods and Applications*, eds. P. Elliott, J. Wakefield, N. Best, and D. Briggs, pp. 393–414, Oxford: Oxford University Press.

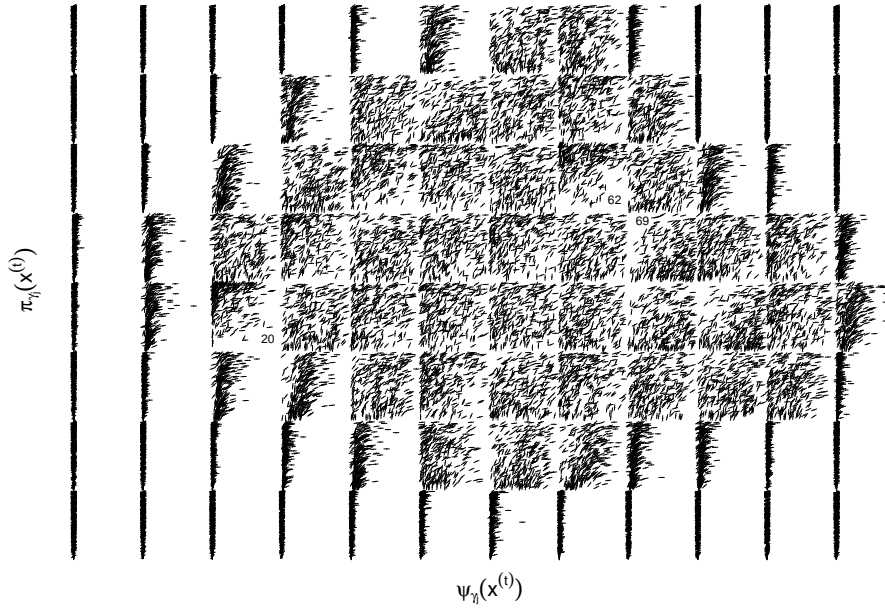


**Figure 4:** The local critique plots for  $\gamma_j$  for SAVIAH3 ( $M = 20000$ , results are shown for a random subsample of size 300). The plots for the latent risk areas are laid out according to the respective locations.

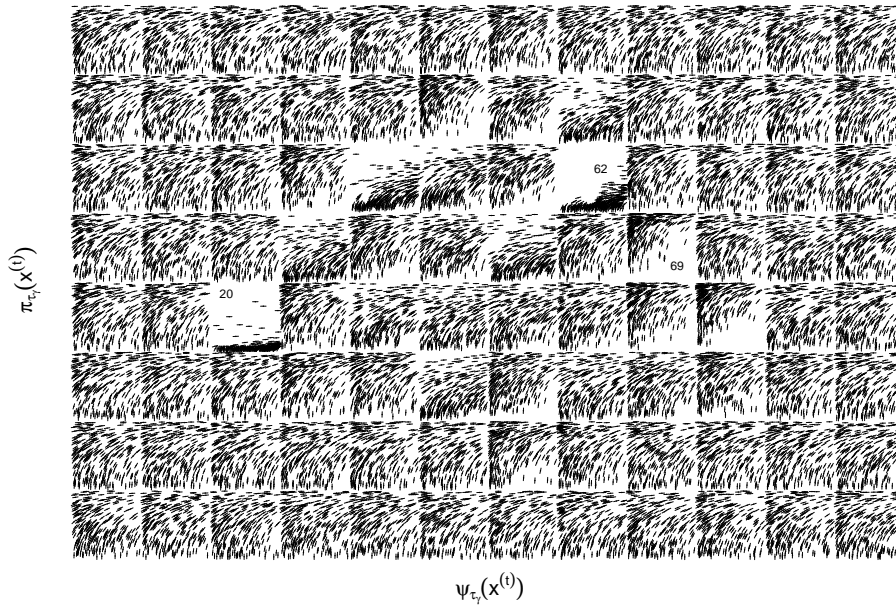


**Figure 5:** The local critique plots for  $\tau_{\gamma,j}$  for SAVIAH3 ( $M = 20000$ , results are shown for a random subsample of size 300). The plots for the latent risk areas are laid out according to the respective locations.